Available online at www.sciencedirect.com

SCIENCE DIRECT

Biochimica et Biophysica Acta 1668 (2005) 158–163

BIOCHIMICA ET BIOPHYSICA ACTA BBA

http://www.elsevier.com/locate/bba

Detection of motional heterogeneities in lipid bilayer membranes by dual probe fluorescence correlation spectroscopy

Jonas Korlach[a], Tobias Baumgart[a], Watt W. Webb[a], Gerald W. Feigenson[b,*]

[a]*School of Applied and Engineering Physics, Cornell University, Ithaca, NY 14853, USA*
[b]*Field of Biophysics, Cornell University, Ithaca, NY 14853, USA*

Received 10 July 2004; received in revised form 14 November 2004; accepted 22 November 2004
Available online 19 January 2005

Abstract

We report the detection of heterogeneities in the diffusion of lipid molecules for the three-component mixture dipalmitoyl-PC/dilauroyl-PC/cholesterol, a chemically simple lipid model for the mammalian plasma membrane outer leaflet. Two-color fluorescence correlation spectroscopy (FCS) was performed on giant unilamellar vesicles (GUVs) using fluorescent probes that have differential lipid phase partition behavior—DiO-C18:2 favors disordered fluid lipid phases, whereas DiI-C20:0 prefers spatially ordered lipid phases. Simultaneously-obtained fluorescence autocorrelation functions from the same excitation volume for each dye showed that, depending on the lipid composition of this ternary mixture, the two dyes exhibited different lateral mobilities in regions of the phase diagram with previously proposed submicroscopic two-phase coexistence. In one-phase regions, both dyes reported identical diffusion coefficients. Two-color FCS thus may be detecting local membrane heterogeneities at size scales below the optical resolution limit, either due to short-range order in a single phase or due to submicroscopic phase separation.

Keywords: Fluorescence correlation spectroscopy; Membrane phase behavior; Lipid bilayer phase diagram; Ternary lipid mixture

1. Introduction

Biomembrane heterogeneities have been implicated in many important cellular functions. The raft hypothesis of current cell membrane biology describes lipid microdomains enriched in long chain saturated lipids and cholesterol that play essential roles in membrane component sorting, membrane signaling and trafficking [1–5]. The existence and involvement of rafts in fundamental biological membrane processes have mostly been inferred using indirect methods, such as detergent extraction and cholesterol depletion [6] of cell membranes, leaving the underlying physicochemical principles of the formation and dynamics of the putative membrane rafts far from being understood [6–8]. Due to these difficulties in defining raft formation and function, model membrane systems have recently gained increased interest [9], using a variety of biophysical techniques, such as wide-field, confocal and two-photon fluorescence microscopy, fluorescence correlation spectroscopy (FCS), fluorescence resonance energy transfer, and excimer formation [10–14].

Methods are needed to characterize dynamic (transient) nonrandom lipid mixing within single phases or coexistence of small, compositionally distinguishable domains [15]. Fluorescence correlation spectroscopy (FCS) [16–18] can be used to study lateral tracer diffusion of membrane markers as a function of membrane composition [19,10], and was recently applied to characterize diffusion in giant unilamellar vesicles (GUVs) with microscopically visible fluid/fluid phase coexistence [20].

To detect submicroscopic biomembrane heterogeneities in the diffusion of lipid molecules in a model membrane system, we describe the application of dual color FCS on

* Corresponding author. 201 Biotechnology Building, Cornell University, Ithaca, NY 14853, USA. Tel.: +1 607 255 4744; fax: +1 607 255 2428.
E-mail address: gwf3@cornell.edu (G.W. Feigenson).

0005-2736/$ - see front matter © 2005 Elsevier B.V. All rights reserved.
doi:10.1016/j.bbamem.2004.11.016

GUVs using fluorescent probes with differential lipid phase partition behavior. Simultaneous autocorrelation curves from the same excitation volume were recorded for DiO-C18:2 which favors disordered lipid phases, and DiI-C20:0 which prefers spatially ordered lipid environments. Probe partitioning was investigated as a means to obtain reporter molecules for motional heterogeneities on a spatial scale smaller than the light microscopy resolution limit. Such probes should recognize differing environments if they are known to be enriched in certain lipid phases and if their diffusion coefficients are sufficiently different in those phases [21].

2. Materials and methods

GUVs were prepared as described [10], with the modifications that DiO-C18:2 (Molecular Probes, Eugene OR) was chosen as the fluid phase lipid probe due to its relatively high photostability. GUV-forming films were incubated at 50 °C for 12 h, and then slowly cooled to room temperature over 4 h. The dye concentrations were 2.5×10^{-5} mol fraction (relative to total lipid). Approximately 5 μl of GUV suspension was placed onto a microscope slide, previously cleaned in 5% KOH/ethanol for 1 min and surrounded by a ring of Apiezon L grease (Structure Probe Inc., West Chester, PA). A coverslip was overlaid with enough pressure to form a thin film of solution sealed to prevent evaporation. The vesicles were allowed to settle for 15 min before the start of an FCS measurement. Measurements were carried out at room temperature (23 °C).

Lipid compositions are expressed as $\chi_{chol}=n_{chol}/(n_{DLPC}+n_{DPPC}+n_{chol})$ and $\chi^{PC}_{DPPC}=n_{DPPC}/(n_{DLPC}+n_{DPPC})$, where n_i refers to the number of moles of component i [12]. DiI-C20:0 favors the ordered membrane phases of DPPC over coexisting fluid phases, while DiO-C18:2 shows opposite partitioning, with partition coefficients for both probes of ~4 (Feigenson and Buboltz, unpublished results).

FCS was performed using the 488 nm line of an argon ion laser, overfilling a 60×, 1.2 NA water immersion microscope objective (Olympus UPlanApo, Melville, NY) on an upright microscope (BX50WI, Olympus) with combined wide-field imaging and FCS capabilities. A GUV was first located with an intensified CCD camera (Stanford Photonics, Palo Alto, CA) by wide-field illumination. After switching to the FCS mode, the laser focus was positioned onto the top central membrane region of the GUV. Excitation intensities at the sample were kept low at ~500 W/cm^2 to avoid a significant population of the triplet state. Fluorescence was collected by the same objective and passed through a dichroic mirror and emission filter (DCLP 488/NIR5 and HQ580/150, Chroma, Brattleboro, VT) to block reflected laser light. Fluorescence from the two different dyes was separated by a dichroic mirror (DCSP 530) and further restricted by two emission filters to minimize bleedthrough (HQ515/30 for DiO channel, HQ580LP for DiI channel, Chroma) before coupling into two 100 μm core diameter fibers (OZ Optics Ltd., Carp, Ontario), each connected to an avalanche photodiode (PE

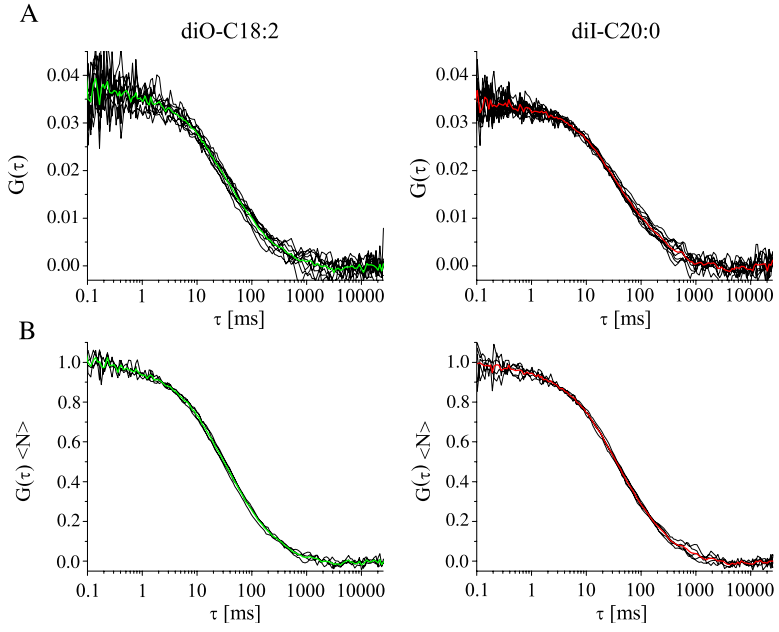

Fig. 1. Dual probe FCS measurements on GUVs. The lipid composition for this example was $\chi^{PC}_{DPPC}=0.625$ and $\chi_{chol}=0.3$. (A) Ten successive autocorrelation curves obtained simultaneously from a single vesicle in the two detection channels for DiO-C18:2 (left) and DiI-C20:0 (right), together with their respective averages (colored curves). The range of diffusion variation from individual 30 s runs was on the order of ~25–50% standard deviation (S.D.). (B) Averaged and normalized autocorrelation curves from all five GUVs measured for this composition, together with their respective averages (colored curves) which were used for the diffusion analysis shown in Fig. 3. Vesicle to vesicle variations were ~10–25% S.D. for all lipid compositions.

Optoelectronics, Fremont, CA) for dual channel autocorrelation recordings (Flex410R, Correlator.com, Bridgewater, NJ). Bleedthrough was negligible in the DiO channel and ~15% in the DiI channel. No bleedthrough correction was carried out; at the illumination intensities used here, this bleedthrough did not result in interpretable correlation curves in control experiments involving DiO-C18:2 alone. At least five separate GUVs were measured for each lipid composition. Ten successive autocorrelation curves of 30 s duration each, obtained simultaneously from a single vesicle in the two detection channels for DiO-C18:2 and DiI-C20:0, were averaged before fitting (Fig. 1A). Small stochastic differences in relative probe concentrations in different GUVs were observed, resulting in different autocorrelation amplitude (~15% around the average $G(0)$ value). To facilitate a comparison of residence times of the fluorescent probes between vesicles of a single sample (Fig. 1B) and between different lipid compositions (Fig. 2), the average correlation curves were normalized to $G(0)=1$.

Autocorrelation curves were fit using a model for the correlation function $G(\tau)$ of two-dimensional diffusion in an excitation volume of Gaussian intensity distribution, $I(r)=I_0 e^{-r^2}/w^2$ (beam waist at focal point w), in the absence of triplet state formation [17,18,22]:

$$G(\tau) = \frac{1}{N} \cdot \frac{1}{1 + 4D\tau/w^2} \qquad (1)$$

where N is the average number of molecules in the focal area, and D is the diffusion coefficient of the fluorescent lipid probe.

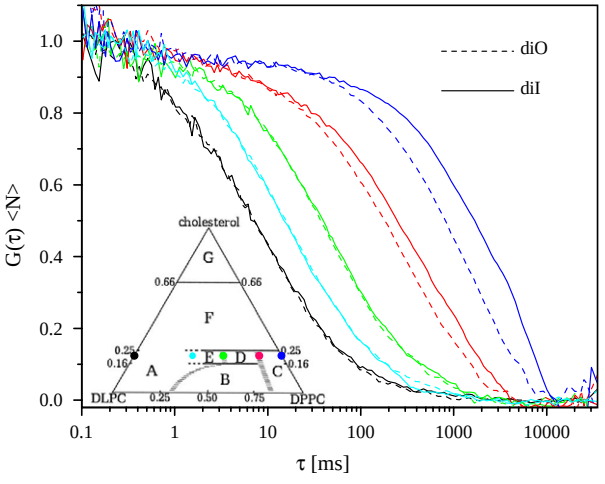

Fig. 2. Autocorrelation curves of DiI-C20:0 (solid) and DiO-C18:2 (dashed) for different DPPC/DLPC compositions at constant χ_{chol}=0.2. χ^{PC}_{DPPC} values were 0, 0.4, 0.625, 0.8, and 1.0 (from left to right). The inset shows the corresponding compositions on the published DLPC/DPPC/cholesterol phase diagram (phase designations are: (A) DLPC-rich fluid lamellar phase; (B) coexisting fluid lamellar phase and DPPC-rich ordered phase; (C) DPPC-rich ordered phase; (D) a single phase that changes continuously from a rigid ordered phase at the C/D boundary to a fluid-ordered phase at the D/E boundary; (E) a fluid-ordered phase; (F) a fluid-ordered phase different from E; (G) coexisting crystalline cholesterol monohydrate and a cholesterol-saturated lamellar phase, from [12]).

3. Results

The dual channel detection FCS setup allowed to record independently the diffusional motion of the two different lipid probes, DiO-C18:2 and DiI-C20:0. Immobilization of the vesicles on the bottom coverglass surface was essential for reliable data acquisition. The sample preparation protocol described here resulted in a glass surface to which the GUVs adhered sufficiently well to permit successful measurements for all sample compositions.

Fig. 1A shows an example of ten autocorrelation curves measured consecutively on a single GUV from the two detection channels (black traces), together with their respective averages (colored traces). The range of variation from individual 30 s runs, determined from fits to individual runs, was on the order of ~25–50% standard deviation (S.D.) around the average diffusion coefficient.

Averaged autocorrelation curves from separate vesicles were normalized, and their average was calculated for the fitting and determination of diffusion coefficients (Fig. 1B). Autocorrelation curves were similar for all vesicles in a given sample, permitting reliable independent assignments of the probe diffusional properties within their respective microenvironment as a function of lipid composition. Variations in D obtained from separate GUVs at a given lipid composition were ~10–25% S.D. of the average diffusion coefficient value shown in Fig. 3.

FCS analysis was performed at 23 °C in the DLPC/DPPC/cholesterol phase diagram, along two DLPC/DPPC composition lines at constant molar fractions of cholesterol at χ_{chol}=0.2 and χ_{chol}=0.3. Earlier studies showed that at χ_{chol}=0.2, the bilayer revealed no macroscopic phase separation detectable by confocal fluorescence microscopy [12]. But at this cholesterol concentration from χ^{PC}_{DPPC}=0.62–0.85, dipyrene-PC excimer/monomer ratios, as well as FRET between DiO-C18:2 and DiI-C20:0, indicated a boundary. This region could perhaps be described as a continuous phase transition, or by a coexistence of phases with domain dimensions smaller than the optical resolution limit. For χ^{PC}_{DPPC}>0.85, two-phase coexistence of liquid-ordered and spatially ordered phases has been described [23]. Earlier studies showed no clear indication of a phase transition at χ_{chol}=0.3.

Depending on the lipid composition of this ternary mixture, differences in the diffusion behavior were observed for these two fluorescent lipid probes with different partitioning characteristics. The most drastic effects of differential probe diffusion as a function of composition were observed at high DPPC concentrations for χ_{chol}=0.2 (Fig. 2). Autocorrelation curves of the two probes were identical in a region spanning from χ^{PC}_{DPPC}=0 to 0.8. With χ^{PC}_{DPPC}>0.8, the diffusion of DiI-C20:0 was two- to threefold slower than for DiO-C18:2, resulting in a split between the autocorrelation curves from the two probes (Fig. 2).

Within the accuracy of the measurements, in all GUVs composed of lipid compositions corresponding to one-

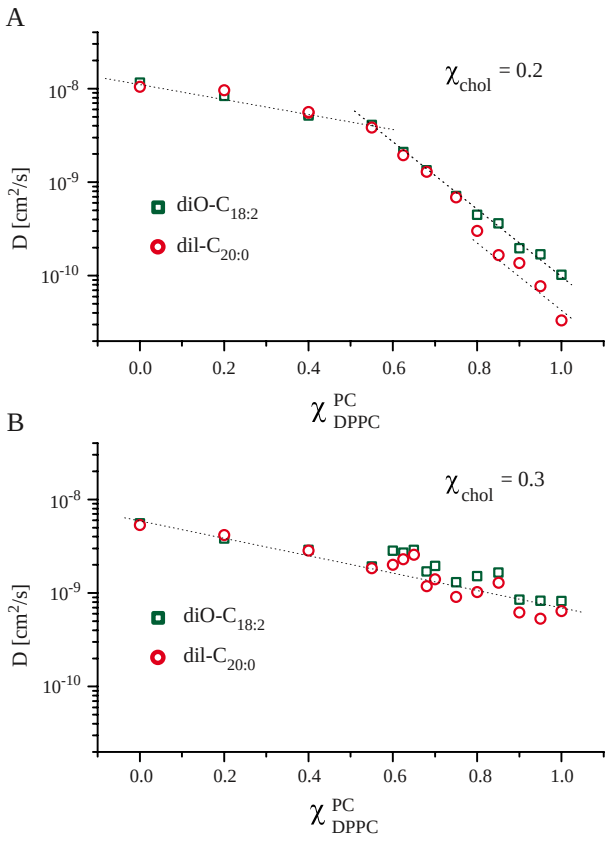

Fig. 3. Diffusion coefficients of DiO-C18:2 (red) and DiI-C20:0 (green) as a function of DPPC/DLPC composition for constant (A) χ_{chol}=0.2 and (B) χ_{chol}=0.3. The thin dotted lines are guides for the eye to visualize trends described in the text. Uncertainties in D values were on the order of 10–25% for all compositions; the corresponding error bars are omitted from the graphs for clarity. (For interpretation of the references to colour in this figure legend, the reader is referred to the web version of this article.)

phase compositional regions, both dyes exhibited indistinguishable diffusion behavior, and an identical dependence on membrane composition. Most autocorrelation curves could be described well by a single component, two-dimensional diffusion model (Eq. (1)). For some individual GUVs, a model with two different diffusing species or anomalous diffusion was required to obtain a satisfactory fit (R^2>0.999). However, no correlation between a particular region in the phase diagram and the goodness of fit to a single component, two-dimensional model was observed. Diffusion coefficients from fits to the one-component, two-dimensional diffusion model as a function of lipid composition are shown in Fig. 3.

Across the DLPC/DPPC composition at χ_{chol}=0.2, the diffusion of both probes slowed down by a factor of ~3 between χ^{PC}_{DPPC}=0–0.55, and then more steeply (by a factor of ~50–100) from χ^{PC}_{DPPC}=0.55–1.0 (Fig. 3A, dashed guides). Both diffusion coefficients spanned a range of almost three orders of magnitude across the entire DPPC/DLPC composition. In the region of motional heterogeneity (χ^{PC}_{DPPC}=0.8–1.0), the dependences of diffusion coefficients on lipid composition for the two probes was very similar, resulting in parallel trends in the graph (dashed guides).

For χ_{chol}=0.3 at χ^{PC}_{DPPC}=0–0.6 (Fig. 3B), the diffusion of the two probes was also indistinguishable, as observed for the lower cholesterol concentration χ_{chol}=0.2 (Fig. 3A). The trend of decreasing diffusion coefficients in this χ^{PC}_{DPPC} region was very similar for the two cholesterol concentrations studied, with the diffusion coefficients of both dyes for χ_{chol}=0.3 approximately twofold lower than for χ_{chol}=0.2 (compare D values in Fig. 3A and B at χ_{DPPC}^{PC}=0–0.6). At higher χ_{DPPC}^{PC} values at χ_{chol}=0.3 (Fig. 3B), DiI-C20:0 diffusion was ~1.3 to 1.5-fold slower than DiO-$C_{18:2}$. A somewhat larger variability in the autocorrelation curves determined from vesicles composed of >0.6 was observed, perhaps reflecting a larger variation in the exact lipid composition in individual vesicles which could potentially conceal more subtle phase dependencies. Over the entire DPPC/DLPC composition line at χ_{chol}=0.3, diffusion coefficients varied within approximately one order of magnitude, decreasing logarithmically with increasing DPPC.

Diffusion coefficients were indistinguishable for the two probes along the entire single phase DLPC/cholesterol binary compositional space (χ_{DPPC}^{PC}=0, data not shown). Diffusion slowed down with increasing molar fraction of cholesterol, as described previously for DiI-C20:0 [10].

4. Discussion

Dual probe FCS has been used previously mainly in cross correlation mode for various investigations of molecular interactions (reviewed in [24]). Here, it is demonstrated that two-color FCS can provide a tool to detect motional heterogeneities at a spatial scale below the optical resolution limit.

The observation that the diffusion of these two probes is indistinguishable in the studied homogenous one-phase compositional regions is important with respect to reliable assessments of molecular mobility in the membranes. The calculations of Saffman and Delbrück [25] and subsequent generalizations showed that molecular diffusion in membranes is only weakly dependent on probe dimensions and primarily determined by effective membrane viscosity, supporting the expectation that membrane diffusion properties are independent of the probe used at the low concentrations required to perform FCS, unless the probe selectively interacts with membrane components. In conjunction with the known partition behavior of the fluorescent lipid probes in coexisting equilibrium phases and information about the phase diagram determined by other measurement techniques [12], we find that the submicroscopic environment can be usefully studied by measuring the diffusional mobilities of the probes. More refined experiments and analysis may provide access to the size and temporal dynamics of these nanoscopic domains. Measurements can be combined with temperature control

to determine and characterize phase transitions and critical point phenomena [14].

The two-phase coexistence region at χ_{chol}=0.2, χ^{PC}_{DPPC}>0.6 has been described previously by several laboratories (reviewed in [12]). Dual probe FCS provides dynamic information about this compositional region, showing that diffusion is approximately twofold slower in the spatially ordered phase enriched in DiI-C20:0. Membrane mobility slows down in both phases in a similar manner with increasing χ^{PC}_{DPPC}.

The change of χ_{chol} from 0.2 to 0.3 in the compositional region χ^{PC}_{DPPC}>0.6 eliminates the sudden steep drop in diffusional mobilities with increasing χ^{PC}_{DPPC} (Fig. 3), presumably by decreasing the stability of DPPC-rich nanodomains and thus destroying their spatially ordered phase character, by inducing different, less viscous phase properties, or by preferred partitioning of the dyes along phase boundaries. Thereby the addition of cholesterol in this compositional region enhances diffusional mobility, which is in contrast to the binary mixture of DLPC/cholesterol at 23 °C [26] and DMPC/cholesterol at higher temperatures [27] where increasing cholesterol slows down diffusion in a monotonic manner. It is intriguing that the separation of diffusion coefficients for the two probes by ~50% at χ_{chol}=0.3 coincides with the region of steeper decrease in diffusion coefficients (χ^{PC}_{DPPC}=~0.6–1) at χ_{chol}=0.2. At χ_{chol}=0.2, the sharp decrease of the slope of diffusion coefficients with χ^{PC}_{DPPC} begins at 0.6, but the separation of the two probe diffusion coefficients by ~100% only spans the range χ^{PC}_{DPPC}~0.8–1, suggesting an intersection of two different transitions.

The observation that diffusion coefficients between the two probes are slightly separated at χ_{chol}=0.3 and χ^{PC}_{DPPC}=~0.6–1 implies that nanoscopic motional heterogeneities may persist in this region previously determined as L_o [12]. The experiments performed here were carried out at low illumination intensities to avoid triplet state formation and photobleaching over the entire range of all diffusion coefficients measured. To investigate specific areas of the phase diagram, such as this region with possible nanoscopic domain character, excitation intensities could be increased for higher signal-to-noise in the autocorrelation curves and greater confidence in diffusion dynamics assignments. Because submicroscopic biomembrane heterogeneities have been implicated in many important cellular functions, this method may also provide a valuable technique to characterize the dynamics of these nanoscopic domains in living cells.

Acknowledgements

This research was performed in the Developmental Resource for Biophysical Imaging Opto-Electronics and was made possible by Grant Number 9 P41 EB001976-16 from the National Institute of Biomedical Imaging and Bioengineering (NIBIB) and the National Center for Research Resources (NCRR), National Institutes of Health, and by Grant Number MCB-0315330 from the National Science Foundation (to G.W.F.).

References

[1] K. Simons, E. Ikonen, Functional rafts in cell membranes, Nature 387 (1997) 569–572.
[2] D.A. Brown, E. London, Functions of lipid rafts in biological membranes, Annu. Rev. Cell Dev. Biol. 14 (1998) 111–136.
[3] E. Ikonen, Roles of lipid rafts in membrane transport, Curr. Opin. Cell Biol. 13 (2001) 470–477.
[4] H. Sprong, P. Sluijs, G. van Meer, How proteins move lipids and lipids move proteins, Nat. Rev., Mol. Cell Biol. 2 (2001) 504–513.
[5] F.R. Maxfield, Plasma membrane microdomains, Curr. Opin. Cell Biol. 14 (2002) 483–487.
[6] M. Edidin, The state of lipid rafts: from model membranes to cells, Annu. Rev. Biophys. Biomol. Struct. 32 (2003) 257–283.
[7] H. Heerklotz, Triton promotes domain formation in lipid raft mixtures, Biophys. J. 83 (2002) 2693–2701.
[8] S. Munro, Lipid rafts: elusive or illusive? Cell 115 (2003) 377–388.
[9] J.R. Silvius, Role of cholesterol in lipid raft formation: lessons from lipid model systems, Biochim. Biophys. Acta 1610 (2003) 174–183.
[10] J. Korlach, P. Schwille, W.W. Webb, G.W. Feigenson, Characterization of lipid bilayer phases by confocal microscopy and fluorescence correlation spectroscopy, Proc. Natl. Acad. Sci. 96 (1999) 8461–8466.
[11] C. Dietrich, L.A. Bagatolli, Z.N. Volovyk, N.L. Thompson, M. Levi, K. Jacobson, E. Gratton, Lipid rafts reconstituted in model membranes, Biophys. J. 80 (2001) 1417–1428.
[12] G.W. Feigenson, J.T. Buboltz, Ternary phase diagram of dipalmitoyl-PC/dilauroyl-PC/cholesterol: nanoscopic domain formation driven by cholesterol, Biophys. J. 80 (2001) 2775–2788.
[13] S.L. Veatch, S.L. Keller, Organization in lipid membranes containing cholesterol, Phys. Rev. Lett. 89 (2002) 268101-1–268101-4.
[14] T. Baumgart, S.T. Hess, W.W. Webb, Imaging coexisting fluid domains in biomembrane models coupling curvature and line tension, Nature 425 (2003) 821–824.
[15] J. Huang, G.W. Feigenson, Monte Carlo simulation of lipid mixtures: finding phase separation, Biophys. J. 65 (1993) 1788–1794.
[16] E.L. Elson, D. Magde, Fluorescence correlation spectroscopy: 1. Conceptual basis and theory, Biopolymers 13 (1974) 1–27.
[17] D. Magde, E.L. Elson, W.W. Webb, Fluorescence correlation spectroscopy: 2. Experimental realization, Biopolymers 13 (1974) 29–61.
[18] D. Magde, W.W. Webb, E. Elson, Thermodynamic fluctuations in a reacting system—measurement by fluorescence correlation spectroscopy, Phys. Rev. Lett. 29 (1972) 705.
[19] P.F. Fahey, D.E. Koppel, L.S. Barak, E.L. Elson, W.W. Webb, Lateral diffusion in lipid bilayers, Science (1977) 305–306.
[20] N. Kahya, D. Scherfeld, K. Bacia, B. Poolman, P. Schwille, Probing lipid mobility of raft-exhibiting model membranes by fluorescence correlation spectroscopy, J. Biol. Chem. 278 (2003) 28109–28115.
[21] U. Meseth, T. Wohland, R. Rigler, H. Vogel, Resolution of fluorescence correlation measurements, Biophys. J. 76 (1999) 1619–1631.
[22] P. Schwille, J. Korlach, W.W. Webb, Fluorescence correlation spectroscopy with single-molecule sensitivity on cell and model membranes, Cytometry 36 (1999) 176–182.
[23] T.P.W. McMullen, R.N. McElhaney, New aspects of the interaction of cholesterol with dipalmitoylphosphatidylcholine bilayers as revealed by high-sensitivity differential scanning calorimetry, Biochim. Biophys. Acta, Biomembr. 1234 (1995) 90–98.

[24] R. Rigler, E. Elson, Fluorescence correlation spectroscopy: theory and applications, Springer, Berlin, 2001.
[25] P.G. Saffman, M. Delbrück, Brownian motion in biological membranes, Proc. Natl. Acad. Sci. U. S. A. 72 (1975) 3111–3113.
[26] J. Korlach, P. Schwille, W.W. Webb, G.W. Feigenson, Characterization of lipid bilayer phases by confocal microscopy and fluorescence correlation spectroscopy, Proc. Natl. Acad. Sci. U. S. A. 96 (1999) 8461–8466.
[27] J.L. Rubenstein, B.A. Smith, H.M. McConnell, Lateral diffusion in binary mixtures of cholesterol and phosphatidylcholines, Proc. Natl. Acad. Sci. U. S. A. 76 (1979) 15–18.